Front. Environ. Sci. Eng. 2018, 12(1): 5
https//doi.org/10.1007/s11783-017-1003-x

RESEARCH ARTICLE

Degradation of Azo dye direct black BN based on adsorption and microwave-induced catalytic reaction

Shanshan Ding[1], Wen Huang[1], Shaogui Yang (✉)[2], Danjun Mao[1], Julong Yuan[1], Yuxuan Dai[1], Jijie Kong[1], Cheng Sun[1], Huan He (✉)[2], Shiyin Li[2] Limin Zhang[2]

1 State Key Laboratory of Pollution Control and Resource Reuse, School of the Environment, Nanjing University, Nanjing 210023, China
2 School of Environment, Nanjing Normal University, Nanjing 210023, China

HIGHLIGHTS

- The adsorption behavior of DB BN on microwave catalyst $MgFe_2O_4$-SiC was investigated and the effects of concentration, temperature and pH on the adsorption process were discussed in this study.
- The microwave-induced catalytic degradation rate of DB BN decreased even more than ten percent after the adsorption equilibrium were attained.
- The degradation intermediate products of DB BN were identified and analyzed by GC-MS and LC-MS.
- The proposed degradation pathways of direct black BN (DB BN) were described by combining with the microwave-induced catalytic reaction mechanism of $MgFe_2O_4$-SiC.

GRAPHIC ABSTRACT

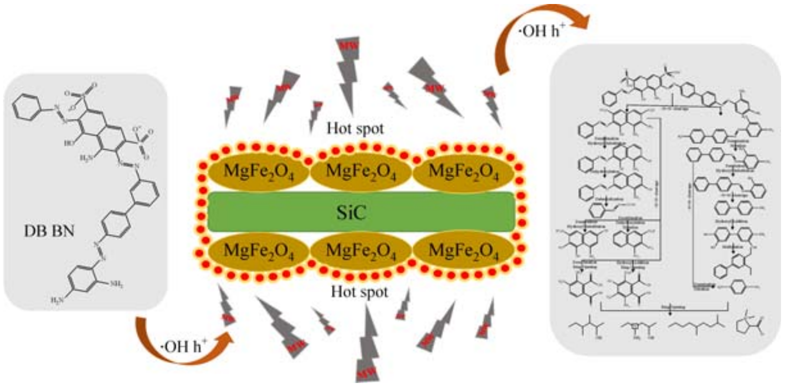

ARTICLE INFO

Article history:
Received 2 March 2017
Revised 3 May 2017
Accepted 15 August 2017
Available online 15 October 2017

Keywords:
Adsorption
Microwave-induced catalytic degradation
Direct black BN
Degradation pathway

ABSTRACT

The novel microwave catalyst $MgFe_2O_4$-SiC was synthesized via sol-gel method, to remove azo dye Direct Black BN (DB BN) through adsorption and microwave-induced catalytic reaction. Microwave-induced catalytic degradation of DB BN, including adsorption behavior and its influencing factors of DB BN on $MgFe_2O_4$-SiC were investigated. According to the obtained results, it indicated that the pseudo-second-order kinetics model was suitable for the adsorption of DB BN onto $MgFe_2O_4$-SiC. Besides, the consequence of adsorption isotherm depicted that the adsorption of DB BN was in accordance with the Langmuir isotherm, which verified that the singer layer adsorption of $MgFe_2O_4$-SiC was dominant than the multi-layer one. The excellent adsorption capacities of $MgFe_2O_4$-SiC were kept in the range of initial pH from 3 to 7. In addition, it could be concluded that the degradation rate of DB BN decreased over ten percent after the adsorption equilibrium had been attained, and the results from the result of comparative experiments manifested that the adsorption process was not conducive to the process of microwave-induced catalytic degradation. The degradation intermediates and products of DB BN were identified and determined by GC-MS and LC-MS. Furthermore, combined with the catalytic mechanism of $MgFe_2O_4$-SiC, the proposed degradation pathways of DB BN were the involution of microwave-induced ·OH and holes in this catalytic system the breakage of azo bond, hydroxyl substitution, hydroxyl addition, nitration reaction, deamination reaction, desorbate reaction, dehydroxy group and ring-opening reaction.

1 Introduction

In recent years, with the rapid development of the dye manufacturing industry, part of the dye wastewater has been discharged into the water during the production process [1,2], which has caused influence on the water quality and biological living environment. Besides, the dye and its degradation intermediate products with toxicity,

---

✉ Corresponding authors
E-mail: yangdlut@126.com, yangsg@njnu.edu.cn; huanhe@njnu.edu.cn

Special Issue—Advanced Treatment Technology for Industrial Wastewaters (Responsible Editors: Junfeng Niu & Hongbin Cao)

carcinogenicity and mutagenicity can also affect people's normal life. Therefore, the removal of dye pollutants in water has been attracted more and more attention.

Azo dyes have been widely used due to its mature production process with low and stable cost [3], in the area of printing and dyeing, paper, leather, cosmetics, medicine, food and other industries [4,5]. However, azo dyes are resistant to decompose under aerobic conditions and can be long-term stable in the environment [6]. Although they can be reduced by microorganisms to produce aromatic amines and other intermediates under anaerobic conditions, it is difficult for these substances to be decomposed and mineralized in water. The harmfulness and toxicity of these pollutants can also cause great effect on aquatic animals, plants and human health [7].

Nowadays, there are many studies about the treatment methods of dye wastewater, which can be mainly divided into physical method, chemical method, biological method or the optimal combination between them. Among them, researches focuses on the adsorption technology for the treatment of wastewater [8,9]. As is known to all, activated carbon (AC) is the most widely used solid adsorbent in industrial application, because of its high treatment cost and easier loss in treatment process, and the main problem is the regeneration which is the key to suppress the widespread employment of AC. It is well documented that Advanced Oxidation Technology (AOP) can solve these problems mentioned above [10,11], it has been utilized in the treatment of azo dyes wastewater for which the pollutants can be degraded by its non-selective and oxidative reactive groups (such as hydroxyl radicals (·OH)) in the system. In addition, AOP can help the dye quickly decomposed through oxidation. Ultimately, the dye molecules can be mineralized without secondary pollution. As one of the most important technique of AOPs, microwave-induced catalysis is considered to be an very effective technique for the treatment of refractory wastewater, for promoting the progress of the reaction and saving energy [12]. At present, most of the existing studies have shown that photocatalysis can treat contaminants in water effectively [13–15], but high concentrations of dye wastewater can affect the transmission of UV-visible light, which will prevent the light from reaching to the surface of the catalyst, making the application of the photocatalytic technology restrictedly. Notably, the microwave-induced catalytic technology, which is a new decomposed technology based on the microwave "sensitizer" instead of the photocatalyst, is considered to be an effective method for the treatment of dye wastes [16,17]. At the same time, a large amount of researches have been reported that microwave-induced catalysis is an efficient technology in the wastewater treatment [18–21]. Therefore, it is of great theoretical and practical value to study the mechanism of microwave action and the effect of microwave induced catalytic oxidation on the removal of azo dyes. It is helpful that the mechanism elucidates the role of microwave induced catalytic technology in practical engineering applications. Under microwave condition, the catalyst, as a dielectric material, strongly absorbs microwave energy and transferring the absorbed energy will transfer to the surface of catalyst resulting in rapidly heating up its surface. Hot spots will also be generated during this process. In addition, the hot spot increases with the enhancement of microwave absorption capacity [22,23]. During the process of microwave irradiation, it is important that electron hole pairs formed inside the material react with the oxygen and water in the system to produce active radical species such as ·OH for accelerating the removal of pollutants.

The role of catalyst or carriers is significant during the microwave-induced catalytic reaction. The common materials that absorb microwave are ferrite, macromolecules, carbon materials, conductive fibers, etc. Among these materials, the ferrite has been favored by researchers because of its high resistivity and catalytic performance. Besides, different types of ferrite materials have different microwave absorption properties, among which the most studies of spinel ferrite. To consider the excellent microwave absorption capacity of spinel-type ferrite, a large number of studies have shown that ferrite can be suitable for microwave-induced catalytic reaction [24,25]. This type of ferrite is composed with the composite metal oxide which Fe_2O_3 and other iron or rare earth oxides are the main component. In this study, $MgFe_2O_4$ was selected as the representative of the spinel-type ferrite which its own constituent elements of the composition of the salts and ions are less toxic on the environment. Zhang et al. had studied that magnesium ferrite was used in the microwave catalysis with better application, in which the removal of acid magenta was up to 99.8% under the microwave irradiation for 1.5 min [26]. For the choice of carrier material, Carbon material gets the favor of many researchers as a common carrier, for its larger diameter resulting in loading material increasedly. As a kind of microwave absorbing material with strong electrical loss, SiC is one of the frequently-used carrier with good performance for its relatively stable chemical properties, thermal conductivity, porosity and good adsorption capacity. When SiC is used as carrier, the as-prepared composite catalyst has strong interfacial polarization, thus increasing its dielectric constant, which enhances the microwave absorption performance of the catalyst. Therefore, the idea is the ferrite loaded onto the surface of SiC, then obtained supported ferrite will enhance the capacity of microwave absorption, thereby improving its microwave-induced catalytic performance [27,28].

In this study, magnesium ferrite ($MgFe_2O_4$) loaded with silicon carbide (SiC) was selected as the microwave-induced catalyst, and its high microwave-induced catalytic activity efficiency was used to adsorb and degrade direct black BN (DB BN). Besides, the influence factors during the adsorption process were investigated during the adsorption process. In the condition of degradation of DB BN, the effect of adsorption to the microwave-induced catalytic activity had also been investigated. Furthermore, the degradation intermediate products of DB BN were determined and analyzed by a gas chromatography-mass spectrometer (GC-MS) and liquid chromatograph-high-resolution mass spectrometer (LC-HRMS), the degradation pathway within the microwave-induced catalytic system was also proposed here. Based on the obtained results from these experiments, the degradation mechanism of DB BN via microwave-induced catalytic was proposed, which can provide a theoretical basis for further study of the reaction mechanism of microwave-induced catalytic system and give reference value for the wastewater treatment.

2 Materials and methods

2.1 Reagents and materials

Silicon carbide (SiC) was purchased from Yuda Silicon Carbide Co., Ltd. (Jiangsu, China). Direct black BN (DB BN) was obtained from Hop Love Chemical Industry Development Co., Ltd. (Shanghai, China). While Ferric nitrate ($Fe(NO_3)_3 \cdot 9H_2O$, analytical reagent (AR), 99.9 wt.% purity) was bought from Sinopharm Group Chemical Reagent Co., Ltd., magnesium nitrate ($Mg(NO_3)_2 \cdot 6H_2O$, AR, purity 99.9 wt.%) and citric acid (AR, purity 99.9 wt.%) were purchased from Nanjing Chemical Reagent Co., Ltd. and used without further purification. The commercial activated carbon F300D (commercial-AC) was obtained from Calgon Carbon Co., Ltd. (Tianjin, China).

2.2 Preparation of microwave catalyst $MgFe_2O_4$-SiC

In this experiment, $MgFe_2O_4$-SiC was prepared by sol-gel method. The detail preparation process was described as follows [29]: $Fe(NO_3)_3 \cdot 9H_2O$ and $Mg(NO_3)_2 \cdot 6H_2O$ (molar ratio of 1:2) were both dissolved in 100 ml deionized water and stirred sufficiently at 60°C under a water bath condition. When adding a certain amount of citric acid (molar ratio of metal ions to citric acid was 1:4), the temperature was raised to 80°C. After the reaction was continued for 2 h, SiC (the loaded amount of 50%) with a diameter of 40-50 μm was added to the system, keeping constantly stirring until the sol was formed. Then the agitation speed was reduced for the formation of gel. Hereafter, the obtained mixture material was dried at 120°C for 10 h. Finally, in order to obtaining SiC-supported magnesium ferrite ($MgFe_2O_4$-SiC), the dried sample was calcined at 800°C for 2 h in N_2 atmosphere.

2.3 Specific experimental steps

2.3.1 Adsorption test

The adsorption behavior of the as-prepared catalyst and the effect of various factors on the adsorption of DB BN were evaluated by batch adsorption experiments. The solution containing the targeted pollutant was placed in a conical flask, and a certain amount of microwave catalyst $MgFe_2O_4$-SiC (1.5 g/L) was added. Covering and sealing with aluminum foil in order to eliminate the effect of photodegradation. The adsorption experiment was carried out in an air bath thermostat (Putian, THZ-82, China). The setting of influencing factors was set according to their natural concentration range. For DB BN, the initial pH was about 6.86 and the pH of the solution was adjusted with dilute hydrochloric acid (1 M) and sodium hydroxide (0.5 M). During the course of the experiment, 3ml of the sample was taken out at given time intervals. After centrifugation, the concentration of the supernatant was measured by UV-vis spectra. The absorption amount of catalyst at equilibrium was calculated by the following equation:

$$q_e = \frac{(c_0 - c_e)V}{m}, \tag{1}$$

where C_0 and Ce are the initial and equilibrium concentrations (mg/L) of the solution, V is the volume of the solution (L), m is the mass of the catalyst (g).

The adsorption kinetics parameters were obtained by fitting the pseudo-first-order kinetics and pseudo-second-order kinetics. The model equation is as follows:

$$\ln(q_e - q_t) = \ln\ q_e - k_1 t, \tag{2}$$

$$\frac{t}{q_t} = \frac{1}{k_2 q_e^2} + \frac{t}{q_e}, \tag{3}$$

where q_e and q_t correspond to the adsorption capacity (mg/g) at equilibrium and the certain time, respectively. While k_1 is the pseudo-first-order kinetic constant (min^{-1}), k_2 is the pseudo-second-order kinetic constant (g/mg/min).

The adsorption isotherm was used to study the adsorption mechanism of the catalyst during the process of adsorption by using the Langmuir and Freundlich models which the model equation are as follows:

$$\frac{1}{q_e} = \frac{1}{q_m} + \frac{1}{K_L q_m c_e}, \tag{4}$$

$$q_e = K_F C_e^{1/n}, \tag{5}$$

where K_L (L/mg) and q_m (mg/g) are constants of the Langmuir Model and the maximum adsorption capacity of the adsorbent. Where K_F ((mg/g) (L/mg)$^{1/n}$) and n are Freundlich constants representing the adsorption capacity of the adsorbent and the adsorption affinity of the adsorbate.

2.3.2 Microwave-induced catalytic degradation experiments

In this experiment, the microwave-induced catalytic degradation of DB BN was executed in a microwave oven (Huiyan, MG08S, China) at the microwave frequency of 2.45 GHz and power of 800 W. In the batch experiment, 100 mL of the DB BN solution and 0.15 g of the $MgFe_2O_4$-SiC were added to a 250 mL flat-bottomed flask, reacted under microwave action at different reaction times. After centrifugation, the concentration of the solution was measured. The microwave-induced catalytic degradation efficiency was calculated by the formula:

$$\text{Removal}(\%) = (1 - C_t/C_0) \times 100\%, \tag{6}$$

where C_0 is the initial concentration of DB BN, and C_t is the instant concentration at the time of reaction t.

2.4 Analytical methods

2.4.1 Analysis of GC-MS

The products with small molecules in the degradation process of DB BN were determined by the GC-MS equipped with a TG-5SILMS column (30 m × 0.25 mm × 0.25 ×m). The reaction solution (20 mL) was centrifuged and filtered through a 0.22 μm film, and then extracted three times with 15 mL of dichloromethane. After dehydrated with anhydrous sodium sulfate, the obtained organic phase was dried under flowing nitrogen. Subsequently, the sample with TMS derivatization was carried out at 50°C for 1 h with adding 0.2 mL of bis (trimethylsily) trifluoroacetamide (BSTFA). The particular temperature program of the GC-MS was shown as follows: the initial temperature of GC was 40°C for 10 min, and then raised to 100°C at a rate of 12°C/min, following that the temperature raised to 200°C at a rate of 5°C/min, finally the temperature attained to 280°C at 20°C/min and held for 5 min. The carrier gas with high purity helium at the flow rate of 1.0 mL/min was used. EI source was utilized and the election energy was 70 eV, the temperature of ion source was set to 280°C. The tested compounds could be analyzed according to the NIST library.

2.4.2 Analysis of LC-MS

The degradation intermediate products of DB BN were determine and analyzed by the LC-HRMS equipped with Agilent Plus C18 column (3.5 μm, 2.1 mm × 100 mm). Before analysis, the samples treated by the solid phase extraction and rotary evaporation. The mobile phase was a 2% formic acid solution (A) and methanol (B). The detailed gradient was set as follows: $t = 0$ min, A : B = 9: 1 (V/V), $t = 5$ min, A : B = 1 : 1(V/V); $t = 15$ min, A : B = 9 : 1(V/V). The duration of the whole process lasted for 25 min. The mass range was set from 100 to 1000 with the utilization of ESI source, and the injection amount was 10 μL.

3 Results and discussion

3.1 Adsorption kinetics

Figure 1 describes the adsorption kinetics of DB BN on $MgFe_2O_4$-SiC and commercial-AC, where Fig. 1(a) shows the adsorption kinetics with different initial concentrations of DB BN, and Fig. 1(b) depicts the similar adsorption kinetics under different temperatures. In Fig. 1(a), the adsorption capacity of $MgFe_2O_4$-SiC increased rapidly with extension of the adsorption time: it has been clearly seen that the adsorption rate was very fast within 40 min, but when the adsorption time was more than 40 min, the adsorption rate decreased obviously; After the adsorption reaction was carried out for 120 min, the adsorption equilibrium was achieved. Generally, when the adsorption had just begun, more adsorption sites were on the surface of $MgFe_2O_4$-SiC, and the concentration of DB BN was relatively high, these situations were conducive to the occurrence of adsorption; and as the adsorption time went on, effective adsorption sites decreased which caused the adsorption rate reduced; gradually, the dynamic adsorption equilibrium had been achieved. Thus, it could be concluded that the adsorption amount of DB BN on $MgFe_2O_4$-SiC was influenced by the concentration of the solution. Besides, the compared experiment had been executed, which showed that the as-prepared $MgFe_2O_4$-SiC has better adsorption behavior than the commercial-AC. The same phenomenon was also found evidently in Fig. 1(b). Temperature was an important factor affecting the activity of adsorbent in the adsorption process. As shown in Fig. 1(b), the adsorption capacity of the microwave catalyst $MgFe_2O_4$-SiC enhanced slightly with the increase of temperature, indicating that the effect of temperature on the adsorption of the catalyst is less and it was not the decisive factor affecting the adsorption behavior. It was obviously concluded that the concentration and temperature have effect on the adsorption kinetics process and the adsorption capacity. The results are shown in Table 1 using the pseudo-first-order kinetics and the pseudo-second-order kinetics models. It can be investigated from the table that the absorption process of DB BN on $MgFe_2O_4$-SiC were more fit with pseudo-second-order kinetics equation which can be utilized to estimate the adsorption amount of adsorbent under different conditions.

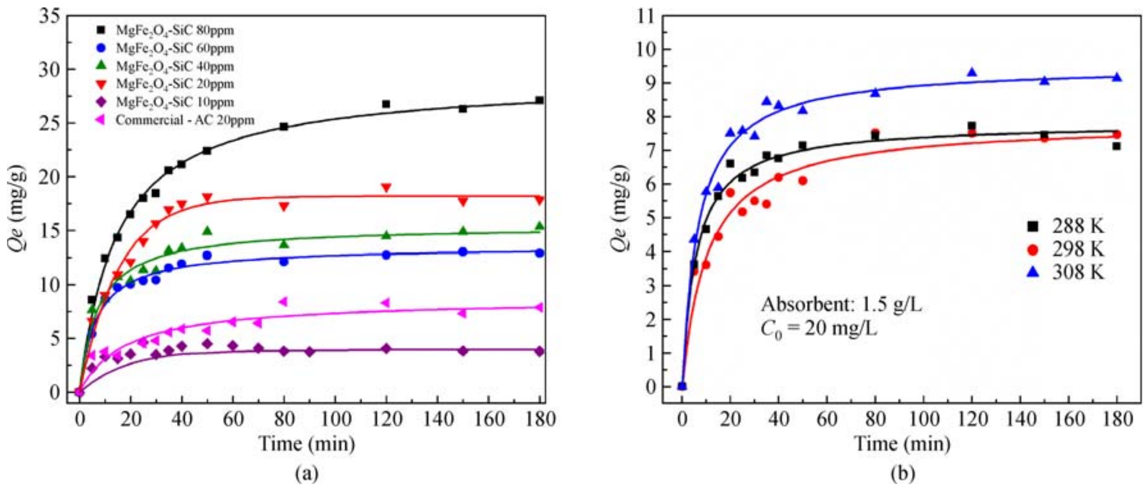

(a) (b)

Fig. 1 (a) The adsorption kinetics of MgFe$_2$O$_4$-SiC and commercial-AC with different initial concentrations of DB BN (adsorbent dosage = 1.5 g/L, T = 298K) and (b) the adsorption kinetics of microwave catalyst MgFe$_2$O$_4$-SiC under different temperatures of the system

Table 1 Parameters of adsorption kinetic models of DB BN onto MgFe$_2$O$_4$-SiC samples

Adsorption condition	Pseudo-first-order equation			Pseudo-second-order equation		
	k_1 (min^{-1})	q_e (mg/g)	R^2	k_2 (g/mg/min)	q_e (mg/g)	R^2
Initial concentration (mg/L)						
10	0.14948	4.03663	0.9035	0.002295012	4.26157	0.8822
20	0.10038	12.2962	0.9643	0.037969	13.5094	0.9870
40	0.08822	14.08029	0.9120	0.051627	15.41989	0.9628
60	0.06549	18.173	0.9802	0.077939	20.1889	0.9644
80	0.05067	25.67526	0.9662	0.16686361	29.07415	0.9941
Temperature (K)						
288	0.10873	7.1567	0.9677	82.38985	7.81218	0.9841
298	0.06472	7.06067	0.8961	46.23871	7.83924	0.9523
308	0.09652	8.67823	0.9539	129.86861	9.51966	0.9837

3.2 Effect of pH on the adsorption capacity of MgFe$_2$O$_4$-SiC

This study was not only discussing the effect of concentration and temperature on the adsorption activity of MgFe$_2$O$_4$-SiC, but also taking pH as an influence factor of adsorption process into consideration [30]. It is well documented that pH is an important factor affecting the surface charge of the adsorbent, and it also has a certain influence on the ionization degree of the dye ion itself [31]. In addition, the competition of the active site of the adsorbent between hydrogen ions and adsorbed ions is also directly related to pH [32,33]. Figure 2(a) depicts the adsorption kinetics of MgFe$_2$O$_4$-SiC with different initial pH of DB BN, which shows from the figure that the adsorption process of DB BN on MgFe$_2$O$_4$-SiC were also fit with pseudo-second-order kinetics equation with different pH. As can be seen from Fig. 2(b), the acidic conditions favored the adsorption of DB BN. It is well-known that when the pH of the solution is below the isoelectric point of the catalyst, the surface of the catalyst is positively charged. Since the isoelectric point of MgFe$_2$O$_4$-SiC was located near the pH value of 3.6 [29], and for the anionic dyes with $\text{pH} < 3$, the surface of MgFe$_2$O$_4$-SiC was positively charge. Thus, the dye molecules were more easily adsorbed on the surface of the material by improving electrostatic gravity, enhancing the removal efficiency of DB BN at this pH range. However, with the alkaline of the solution increased, the material appeared slight negative charge and mildly excluded pollutants via the electrostatic repulsion. Besides, Gao et al. [29] also revealed that MgFe$_2$O$_4$-SiC has the same good adsorption performance as its microwave-induced catalytic one over a wide pH range, so the initial pH of the degraded solution was not regulated.

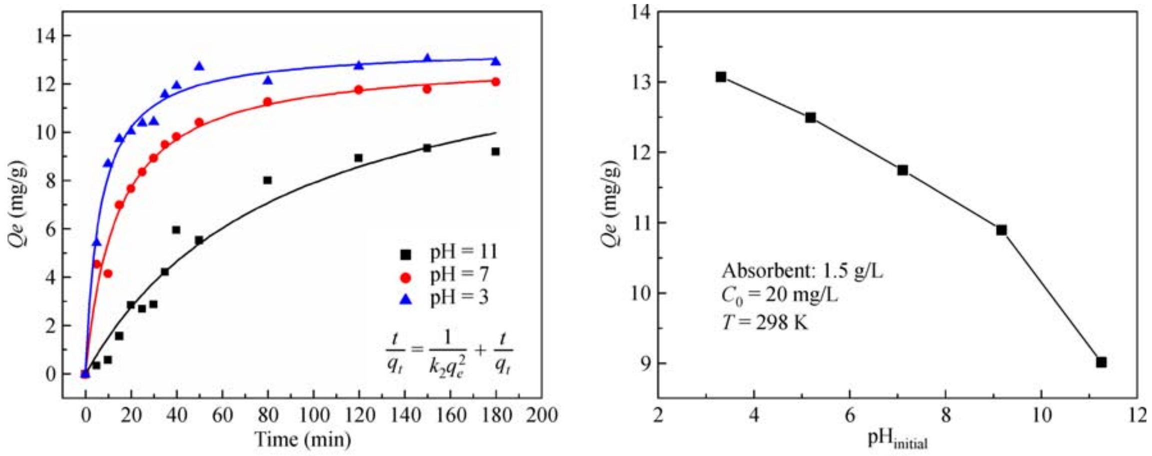

(a) (b)

Fig. 2 (a) The adsorption kinetics of microwave catalyst $MgFe_2O_4$-SiC under different initial pH of DB BN; (b) Effect of pH on the adsorption capacity of microwave catalyst $MgFe_2O_4$-SiC for the removal of DB BN

3.3 Determination of adsorption thermodynamic parameters

The adsorption isotherms were fit with using the Langmuir and Freundlich models and the related parameters are shown in Fig. 3. On the one hand, based on the linear regression coefficient values (R^2 is greater than 0.99), it could be observed that the Langmuir adsorption model of DB BN onto the surface of $MgFe_2O_4$-SiC gave a better fitting than the Freundlich one. On the other hand, the obtained results from the Langmuir model indicated that the adsorption of single layer was more dominant than that of multi-layer in the adsorption process.

3.4 Microwave-induced catalytic degradation of DB BN

To study the microwave-induced catalytic activity of $MgFe_2O_4$-SiC, the degradation of DB BN with different concentrations were studied. As can be depicted in Fig. 4, it indicated that different concentrations of DB BN had a certain degree of degradation within 5 min. Previous studies have shown that DB BN can hardly be degraded under the microwave irradiation alone [29], manifesting that the interaction between the microwave and the catalyst produced a high effect on the degradation of DB BN. On the basis of the results, the DB BN removal efficiency decreased with the increase of initial concentration under microwave-induced catalytic degradation, which was attributed to the restricted active groups. When the specific amount of catalyst was used in the experiment, the number of active groups produced in the reaction system was also tangible. At the lower concentration, the ratio of active groups to DB BN was larger, increasing the chance of DB BN contact with active groups, thus enhancing the catalytic activity. However, when the concentration of target pollutant increased, the decomposition of the

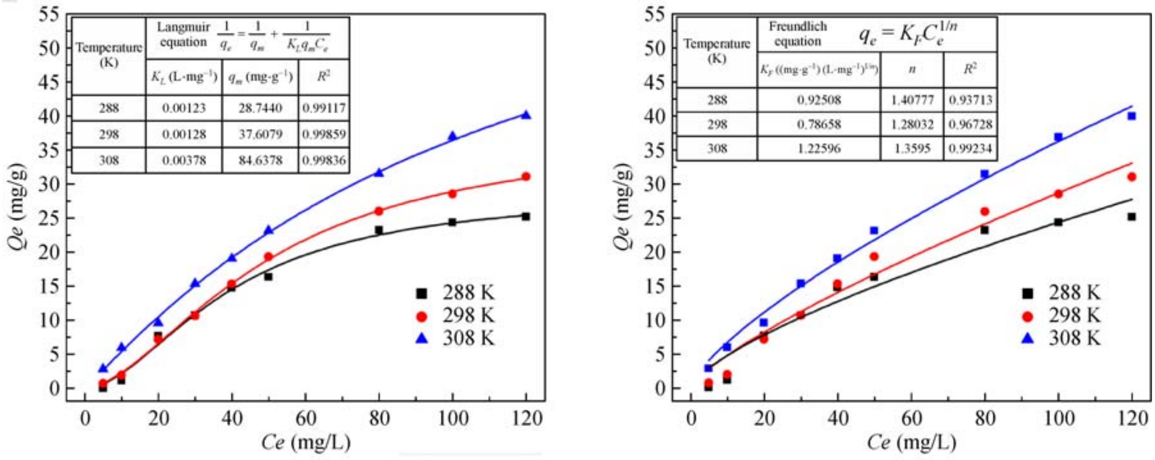

(a) (b)

Fig. 3 Adsorption isotherms of DB BN onto microwave catalyst $MgFe_2O_4$-SiC fitting with (a) Langmuir model; (b) Freundlich model

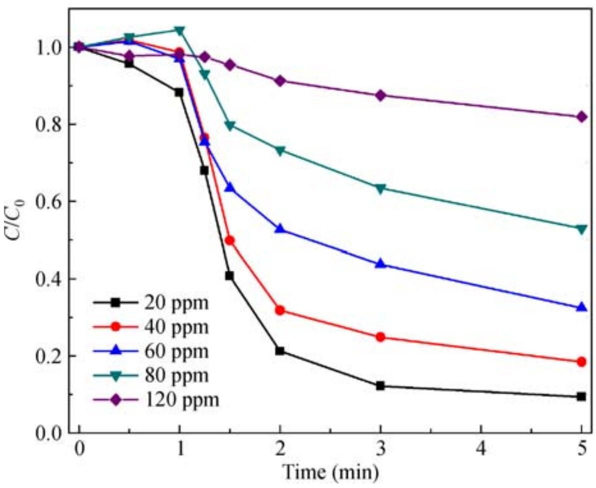

Fig. 4 Microwave-induced catalytic degradation of DB BN with different concentrations

intermediate products could also increase. These intermediates also reacted with free radicals and consumed a lot of free radicals, thus for the decrease of the degradation efficiency of DB BN. In addition, the further exploration about the degradation efficiency on the different kinds of azo dyes in the same the microwave-induced catalytic system had also been investigated (Fig. 5). As can be seen from Fig. 5, three azo dyes were obviously microwave-induced catalytic degraded within 5 min with the presence of $MgFe_2O_4$-SiC. The existing studies also manifested that the microwave-induced catalytic system has excellent degradation on reactive red X-3B and active yellow 2 [29]. Therefore, this microwave-induced catalytic system has a wide range of applicability to the removal of dye molecules, and it is expected to be applied to the treatment of dye wastewater.

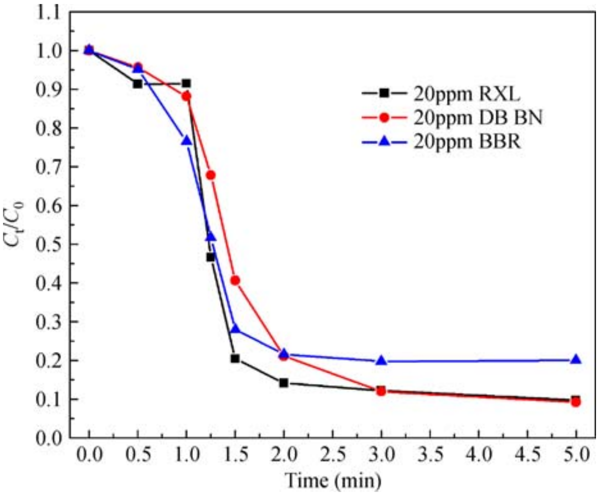

Fig. 5 The degradation of different kinds of azo dyes with $MgFe_2O_4$-SiC under the same microwave-induced catalytic degradation system

3.5 Effect of adsorption on microwave-induced catalytic system

To further investigate the effect of the adsorption behavior of $MgFe_2O_4$-SiC on microwave-induced catalytic degradation process, two situations of the degradation of DB BN with different concentrations under the same microwave-induced catalytic system had been compared: one was microwave-induced catalytic degradation (Fig. 6(a)) without pre-adsorption, and the other was the same degradation after the adsorption equilibrium achieved (Fig. 6(b)). In Fig. 6(b), while five different concentrations of DB BN were tested (20 mg/L, 40 mg/L, 60 mg/L, 80 mg/L, and 120 mg/L) and the microwave-induced catalytic degradation efficiencies were 95%, 88%, 69%, 74% and 68%, the low concentration of DB BN can be completely degraded by the direct microwave-induced catalytic system during the certain time (Fig. 6(a)). In addition, it could be concluded that the degradation rate of DB BN decreased over ten percent after the adsorption equilibrium had been attained. The consequences showed that the direct microwave-induced catalytic degradation system is more favorable for the removal of pollutants. Similar phenomenon happened on the degradation of DB BN on the commercial-AC, there also was the inhibiting effect on the microwave-induced catalytic degradation after the adsorption equilibrium attained. It depicted that the commercial-AC has microwave-induced catalytic activity on the degradation of DB BN which could be attributed to the efficient microwave absorption ability [32,34,35], but it has been faced the poor application especially on the continuous-mode wastewater treatment process for the nonselective adsorption, slow adsorption kinetics and difficult regeneration [23], which the using of $MgFe_2O_4$-SiC could make up for these defects [29]. This may be due to the fact that the catalyst surface adsorbed too much pollutant molecules after the adsorption equilibrium has been reached, which affected the formation of hot spots on the surface of catalyst under microwave irradiation, thus the desorption rate exceeded the formation rate of hot spots to degrade the DB BN, resulting in the suppression of the microwave-induced catalytic degradation process.

3.6 Analysis of degradation products and pathway of DB BN

Under the microwave irradiation, SiC which is known as the typical dielectric can strongly absorb microwave energies. Subsequently, these energies could be quickly transferred to the $MgFe_2O_4$ particles causing the temperature increase of the catalyst surface. In consequence, lots of hot spots were generated on its surface company with the temperature increasing, and the electron hole pairs of $MgFe_2O_4$-SiC were segregated. Hence, the generated electrons and holes can react with O_2 and H_2O in this

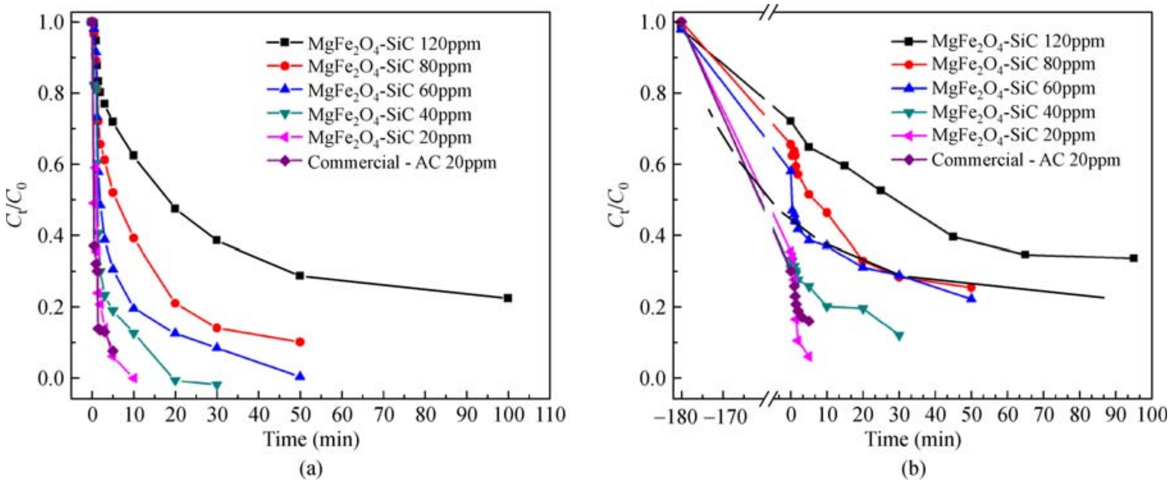

Fig. 6 The pure microwave-induced catalytic degradation of MgFe$_2$O$_4$-SiC and commercial-AC of DB BN (a) without adsorption and (b) after the finished adsorption equilibrium

system to form active species (such as ·OH), which participated in the degradation of DB BN.

The microwave-induced catalytic degradation pathway of the DB BN can be deduced from the analysis of GC-MS and LC-MS analysis (Table 2), as shown in Fig. 7. Compared with the naphthalene and the benzene ring, the azo bond (-*N* = N-) and its adjacent carbon atom in the DB BN molecule were first broken for the required lower

Table 2 Degraded compounds identified by GC-MS and LC-MS

Compounds	Retention time (min)	Chemical structure	Molecular formula	m/z
1	7.41	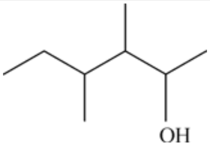	$C_8H_{18}O$	130.23
2	9.36	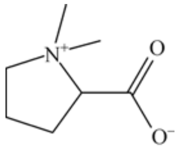	$C_7H_{13}O_2N$	143.21
3	10.47	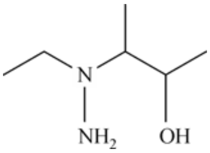	$C_6H_{16}N_2$	116.23
4	13.22	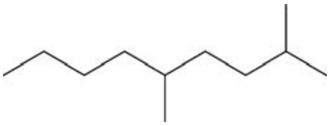	$C_{11}H_{24}$	156.36
5	15.66	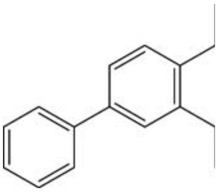	$C_{16}H_{19}$	211.41
6	11.11	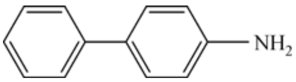	$C_{12}H_9N$	169.15

(*Continued*)

Compounds	Retention time (min)	Chemical structure	Molecular formula	m/z
7	11.84	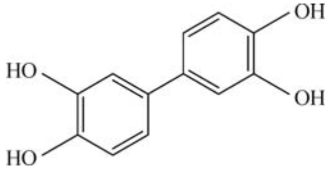	$C_{12}H_{11}NO_3$	217.10
8	12.27	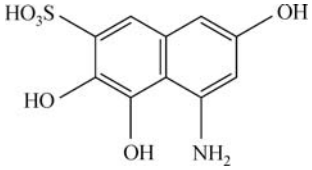	$C_{10}H_9NO_6S$	271.11
9	12.85	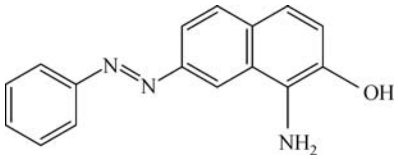	$C_{16}H_{14}N_3O$	262.23
10	13.05	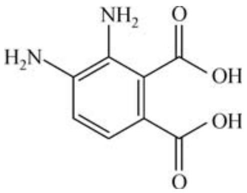	$C_8H_8N_2O_4$	196.18
11	14.31	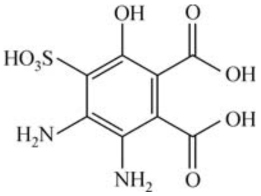	$C_8H_8N_2O_8S$	292.26
12	15.43	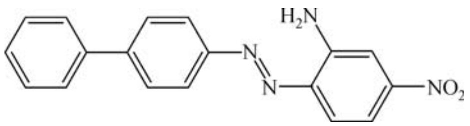	$C_{18}H_{14}N_4O_2$	318.30
13	15.48	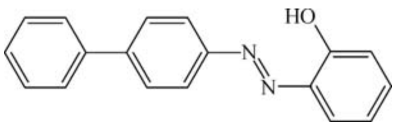	$C_{18}H_{14}N_2O$	274.27
14	16.04		$C_6H_4N_2O_4$	168.07
15	16.70	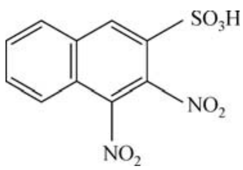	$C_{10}H_6N_2O_7S$	297.21
16	17.88	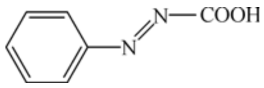	$C_7H_6N_2O_2$	150.02
17	19.13	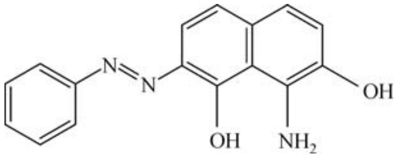	$C_{16}H_{13}N_3O_2$	279.15

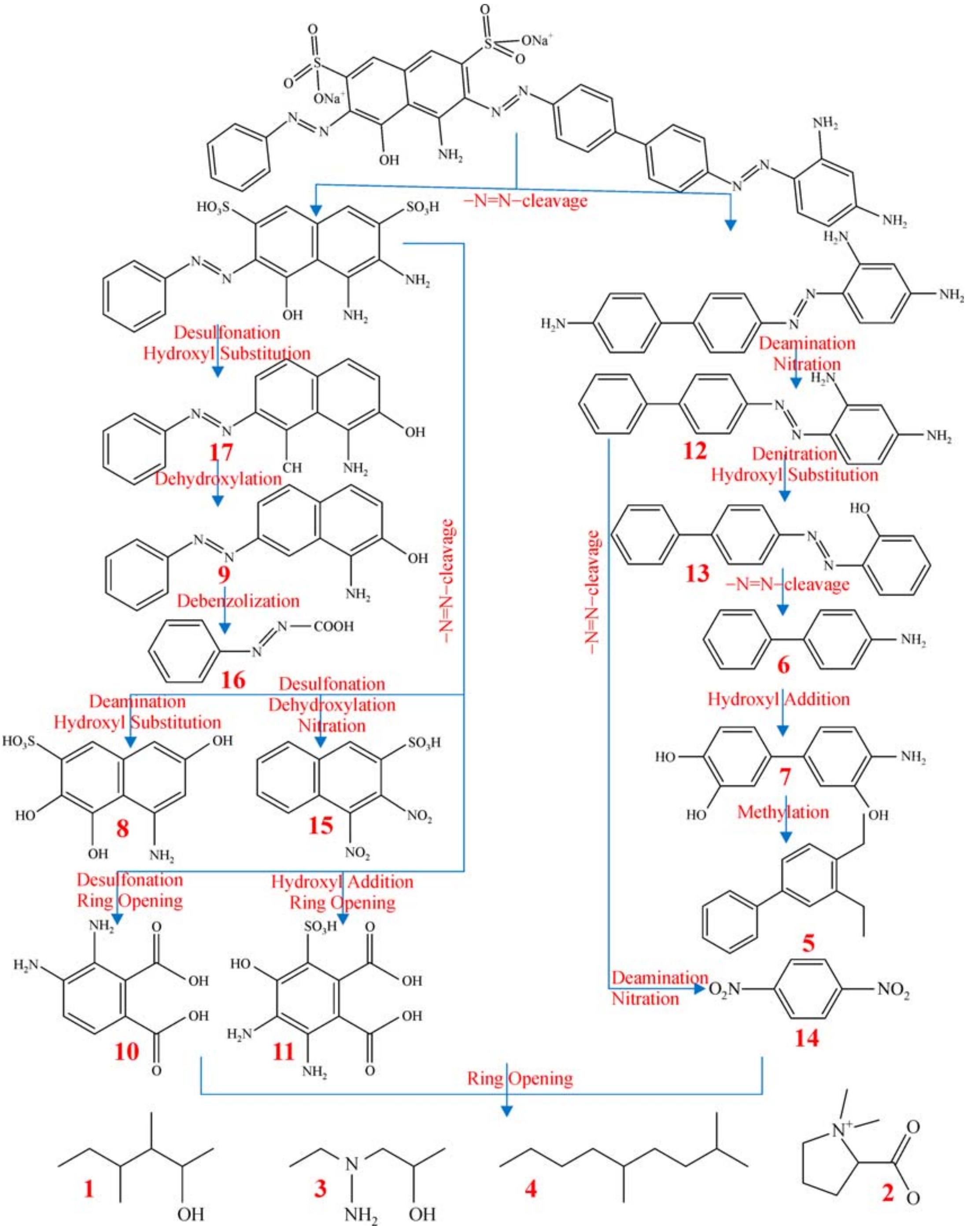

Fig. 7 Possible degradation pathways of DB BN in microwave-induced catalytic system

energy under the action of ·OH, and then two monoazo compounds were formed. Wherein the azo bond of one compound was attached to the biphenyl which was substituted with amino groups, and that of the other compound was attached to the naphthalene ring with multiple functional groups. The former carried on a series of hydroxyl substitution reactions in the presence of ·OH in the system, wherein the compound 17 was a product formed by the desorbate reaction, the compound 9 was then obtained in the dehydroxy group reaction and the compound 16 was the substance formed by the removal of the benzene ring from the compound 9. Obviously, the molecular weight of the products produced throughout the reaction was gradually decreasing. In addition to the degradation pathway described above, on the one hand, the compound linked to the naphthalene ring generated 3,4-dinitronaphthalene-2-sulfonic acid (compound 15) by a series of azo bond breakage, disulfonic acid groups, dehydroxy groups and nitration reactions. On the other hand, based on the breakage of the azo bond, the compound could be degraded by the deionisation and hydroxyl substitution reaction to generate the compound 8. Besides, 3,4-diaminobenzene-1,2-dicarboxylic acid (compound 10) and 3,4-diamino-6-hydroxy-5-benzenesulfono-1,2-dicarboxylic acid (compound 11) obtained under the occurrence of hydroxyl addition, ring-opening reactions and desorbate reaction. Another compound underwent a series of decomposition under the action of hydroxyl groups. Other compound, which was attached to the naphthalene ring with multiple functional groups, underwent a series of decomposition under the presence of ·OH. It was degraded by deamination and nitration reaction to generate the compound 12, and then the compound 13 could be formed by the denitrification and hydroxyl substitution reaction. Subsequently, the azo bond broke, and the resulting 4-aminobiphenyl (compound 6) was further reacted with ·OH to form the compound 7 which contains three hydroxyl groups and was easily replaced by methyl to produce some small molecules. In addition to the degradation pathway described above, the azo bonds in the compound 12 were broken and P-dinitrobenzene (compound 14) was obtained by deamination and nitration reactions. These products underwent ring-opening reactions and were progressively decomposed to produce small molecular substances such as 3,4-dimethyl-2-hexanol (compound 1), (2S)-1,1-dimethylpyrrolidine- 2-formic acid (compound 2), 1-ethyl-1-isobutylhydrazine (compound 3) and 2,5-dimethylnonane (compound 4) which were measured by GC-MS. From the above series of reactions, it can be seen that with the presence of ·OH, the macromolecules of DB BN gradually underwent the breakage of azo bond, hydroxyl substitution reaction, hydroxyl addition reaction, nitration reaction, deamination reaction, desorbate reaction, dehydroxy group reaction and ring-opening reaction, and the DB BN molecule was gradually broken down into some small molecules and finally mineralized to CO_2, H_2O and other innocuous molecules with low molecular mass.

4 Conclusions

In this study, the adsorption and microwave-induced catalytic degradation behaviors of DB BN onto $MgFe_2O_4$-SiC were investigated. The results showed that the catalyst $MgFe_2O_4$-SiC has excellent adsorption effect at initial pH range from 3 to 7. Besides, the adsorption isotherm was in line with Langmuir model, which showed that this was the single layer adsorption process and conformed to the pseudo-second-order dynamics model. Furthermore, two situations of the degradation of DB BN with different concentrations under the same microwave-induced catalytic system had been compared: one was microwave-induced degradation without pre-adsorption equilibrium, and the other was the same degradation after the adsorption equilibrium had been achieved, which indicated that the degradation rate of DB BN decreased over ten percent after the adsorption equilibrium had been attained, and the results from the result of comparative experiments manifested that the adsorption process was not conducive to the process of microwave-induced catalytic degradation. In addition, the microwave-induced catalytic system had good degradation effect on different kinds of azo dyes, and the degradation products of DB BN had been analyzed by GC-MS and LC-MS. Combined with the catalytic mechanism of $MgFe_2O_4$-SiC, the breakage of azo bond, hydroxyl substitution, hydroxyl addition, nitration reaction, deamination reaction, desorbate reaction, dehydroxy group reaction and ring-opening reaction were described to be the degradation pathway of DB BN in this microwave-induced catalytic system.

Acknowledgements This research was financially supported by the Prospective Project on Integration of Industry, Education and Research of Jiangsu Province (BY2016116), National Natural Science Foundation of China (Nos. 21777067 and 51278242) and the Major Science and Technology Program for Water Pollution Control and Treatment of China (No. 2015ZX07204-007).

References

1. Wang H, Zhang L, Chen Z, Hu J, Li S, Wang Z, Liu J, Wang X. Semiconductor heterojunction photocatalysts: Design, construction, and photocatalytic performances. Chemical Society Reviews, 2014, 43(15): 5234–5244
2. Chowdhury S, Balasubramanian R. Graphene/semiconductor nanocomposites (GSNs) for heterogeneous photocatalytic decolorization of wastewaters contaminated with synthetic dyes: A review. Applied Catalysis B: Environmental, 2014, 160: 307–324
3. Rache M L, Garcia A R, Zea H R, Silva A M T, Madeira L M, Ramirez J H. Azo-dye orange II degradation by the heterogeneous Fenton-like process using a zeolite Y-Fe catalyst-Kinetics with a

model based on the Fermi's equation. Applied Catalysis B: Environmental, 2014, 146: 192–200

4. Chang J S, Chou C, Lin Y C, Lin P J, Ho J Y, Hu T L. Kinetic characteristics of bacterial azo-dye decolorization by *Pseudomonas luteola*. Water Research, 2001, 35(12): 2841–2850
5. Saratale R G, Saratale G D, Kalyani D C, Chang J S, Govindwar S P. Enhanced decolorization and biodegradation of textile azo dye Scarlet R by using developed microbial consortium-GR. Bioresource Technology, 2009, 100(9): 2493–2500
6. Han F, Kambala V S R, Srinivasan M, Rajarathnam D, Naidu R. Tailored titanium dioxide photocatalysts for the degradation of organic dyes in wastewater treatment: A review. Applied Catalysis a-General, 2009, 359(1–2): 25–40
7. Engel E, Ulrich H, Vasold R, König B, Landthaler M, Süttinger R, Bäumler W. Azo pigments and a basal cell carcinoma at the thumb. Dermatology (Basel, Switzerland), 2008, 216(1): 76–80
8. Ahmed M A, Brick A A, Mohamed A A. An efficient adsorption of indigo carmine dye from aqueous solution on mesoporous Mg/Fe layered double hydroxide nanoparticles prepared by controlled sol-gel route. Chemosphere, 2017, 174: 280–288
9. He Q, Ni Y, Ye S. Preparation of flowerlike BiOBr/Bi_2MoO_6 composite superstructures and the adsorption behavior to dyes. Journal of Physics and Chemistry of Solids, 2017, 104: 286–292
10. Kusvuran E, Gulnaz O, Irmak S, Atanur O M, Yavuz H I, Erbatur O. Comparison of several advanced oxidation processes for the decolorization of Reactive Red 120 azo dye in aqueous solution. Journal of Hazardous Materials, 2004, 109(1-3): 85–93
11. Pera-Titus M, Garcia-Molina V, Banos M A, Gimenez J, Esplugas S. Degradation of chlorophenols by means of advanced oxidation processes: A general review. Applied Catalysis B: Environmental, 2004, 47(4): 219–256
12. Thostenson E T, Chou T W. Microwave processing: Fundamentals and applications. Composites Part A—Applied Science and Manufacturing, 1999, 30(9): 1055–1071
13. Mao D, Yu A, Ding S, Wang F, Yang S, Sun C, He H, Liu Y, Yu K. One-pot synthesis of BiOCl half-shells using microemulsion droplets as templates with highly photocatalytic performance for the degradation of ciprofloxacin. Applied Surface Science, 2016, 389: 742–750
14. Mao D, Ding S, Meng L, Dai Y, Sun C, Yang S, He H. One-pot microemulsion-mediated synthesis of Bi-rich $Bi_4O_5Br_2$ with controllable morphologies and excellent visible-light photocatalytic removal of pollutants. Applied Catalysis B: Environmental, 2017, 207: 153–165
15. Ding S, Mao D, Yang S, Wang F, Meng L, Han M, He H, Sun C, Xu B. Grapnene-analogue h-BN coupled Bi-rich $Bi_4O_5Br_2$ layered microspheres for enhanced visible-light photocatalytic activity and mechanism insight. Applied Catalysis B: Environmental, 2017, 210: 386–399
16. He H, Yang S, Yu K, Ju Y, Sun C, Wang L. Microwave induced catalytic degradation of crystal violet in nano-nickel dioxide suspensions. Journal of Hazardous Materials, 2010, 173(1–3): 393–400
17. Zhang L, Liu X, Guo X, Su M, Xu T, Song X. Investigation on the degradation of brilliant green induced oxidation by $NiFe_2O_4$ under microwave irradiation. Chemical Engineering Journal, 2011, 173 (3): 737–742
18. Lai T L, Liu J Y, Yong K F, Shu Y Y, Wang C B. Microwave-enhanced catalytic degradation of 4-chlorophenol over nickel oxides under low temperature. Applied Catalysis B: Environmental, 2008, 157(2-3): 496–502
19. Lai T L, Liu J Y, Yong K F, Shu Y Y, Wang C B. Microwave-enhanced catalytic degradation of 4-chlorophenol over nickel oxides under low temperature. Journal of Hazardous Materials, 2008, 157 (2-3): 496–502
20. Lai T L, Lee C C, Wu K S, Shu Y Y, Wang C B. Microwave-enhanced catalytic degradation of phenol over nickel oxide. Applied Catalysis B: Environmental, 2006, 68(3–4): 147–153
21. Remya N, Lin J G. Current status of microwave application in wastewater treatment—A review. Chemical Engineering Journal, 2011, 166(3): 797–813
22. de la Hoz A, Díaz-Ortiz A, Moreno A. Microwaves in organic synthesis. Thermal and non-thermal microwave effects. Chemical Society Reviews, 2005, 34(2): 164–178
23. Chen J, Xue S, Song Y, Shen M, Zhang Z, Yuan T, Tian F, Dionysiou D D. Microwave-induced carbon nanotubes catalytic degradation of organic pollutants in aqueous solution. Journal of Hazardous Materials, 2016, 310: 226–234
24. Xiao J, Fang X, Yang S, He H, Sun C. Microwave-assisted heterogeneous catalytic oxidation of high-concentration Reactive yellow 3 with $CuFe_2O_4$/PAC. Journal of Chemical Technology and Biotechnology (Oxford, Oxfordshire), 2015, 90(10): 1861–1868
25. Shi W, Li Q, An S, Zhang T, Zhang L. Magnetic nanosized calcium ferrite particles for efficient degradation of crystal violet using a microwave-induced catalytic method: Insight into the degradation pathway. Journal of Chemical Technology and Biotechnology (Oxford, Oxfordshire), 2016, 91(2): 367–374
26. Zhang L, Zhou X, Guo X, Song X, Liu X. Investigation on the degradation of acid fuchsin induced oxidation by MgFe2O4 under microwave irradiation. Journal of Molecular Catalysis a-Chemical, 2011, 335(1–2): 31–37
27. Dong L, Qiao J, Yan L, Zheng G, Xiao F. Study on microwave combined with active carbon for treatment of azo-dye wastewater. Environmental Pollution & Control, 2010, 32(4): 34–39
28. Fang X, Xiao J, Yang S, He H, Sun C. Investigation on microwave absorbing properties of loaded $MnFe_2O_4$ and degradation of Reactive Brilliant Red X-3B. Applied Catalysis B: Environmental, 2015, 162: 544–550
29. Gao J, Yang S, Li N, Meng L, Wang F, He H, Sun C. Rapid degradation of azo dye Direct Black BN by magnetic $MgFe_2O_4$-SiC under microwave radiation. Applied Surface Science, 2016, 379: 140–149
30. Sun T, Zhao Z, Liang Z, Liu J, Shi W, Cui F. Efficient As(III) removal by magnetic CuO-Fe_3O_4 nanoparticles through photo-oxidation and adsorption under light irradiation. Journal of Colloid and Interface Science, 2017, 495: 168–177
31. Bulut E, Oezacar M, Sengil I A. Adsorption of malachite green onto bentonite: Equilibrium and kinetic studies and process design. Microporous and Mesoporous Materials, 2008, 115(3): 234–246
32. Zhang Z, Shan Y, Wang J, Ling H, Zang S, Gao W, Zhao Z, Zhang H. Investigation on the rapid degradation of congo red catalyzed by activated carbon powder under microwave irradiation. Journal of

Hazardous Materials, 2007, 147(1-2): 325–333

33. Wang C, Yediler A, Lienert D, Wang Z, Kettrup A. Ozonation of an azo dye C.I. Remazol Black 5 and toxicological assessment of its oxidation products. Chemosphere, 2003, 52(7): 1225–1232
34. Quan X, Zhang Y, Chen S, Zhao Y, Yang F. Generation of hydroxyl radical in aqueous solution by microwave energy using activated carbon as catalyst and its potential in removal of persistent organic substances. Journal of Molecular Catalysis A—Chemical, 2007, 263 (1–2): 216–222
35. Zhang Z, Deng Y, Shen M, Han W, Chen Z, Xu D, Ji X. Investigation on rapid degradation of sodium dodecyl benzene sulfonate (SDBS) under microwave irradiation in the presence of modified activated carbon powder with ferreous sulfate. Desalination, 2009, 249(3): 1022–1029